

# IN-SITU MINERALOGICAL ANALYSIS OF THE VENUS SURFACE USING X-RAY DIFFRACTION AND X-RAY FLUORESCENCE (XRD/XRF).

D.F. Blake<sup>1</sup>, T.S. Bristow<sup>1</sup>, E.B. Rampe<sup>2</sup>, P. Sarrazin<sup>3</sup>, A.H. Treiman<sup>4</sup> and Kris Zacny<sup>5</sup>. <sup>1</sup>NASA Ames Research Center, Moffett Field, CA (david.blake@nasa.gov); <sup>2</sup>NASA Johnson Space Center, Houston, TX; <sup>3</sup>eXaminArt, Mountain View CA; <sup>4</sup>Lunar and Planetary Institute, Houston, TX; <sup>5</sup>HoneyBee Robotics, Pasadena, CA.

**Introduction:** *Quantitative and definitive* mineralogy is critical for elucidating the early history and evolution of Venus, for comparative planetology of the rocky planets, for deducing the potential for habitability on early Venus, and for characterizing Venus as a surrogate for Venus-like exoplanets.

## XRD/XRF analysis of surface regolith will yield:

- Identification of all minerals present >1 wt. %.
- Quantification of all minerals >3 wt. %, including their structure states and cation occupancies.
- Bulk geochemistry of major and minor elements.
- Abundance of all major elements present in each mineral (H and above).
- Valence state of all elements, including speciation of multi-valent species, such as Fe.
- Abundance and composition of X-ray amorphous components, if present.

**The CheMin-V XRD/XRF instrument:** CheMin-V will analyze powdered samples delivered to it inside the pressure shell of the Venus lander by the HoneyBee Robotics Venus drill [1]. CheMin-V is a next-generation XRD/XRF instrument having MSL-CheMin [2] heritage, augmented by enhanced XRD and XRF capabilities. Drilled and powdered Venus regolith is sieved to <150 μm and delivered to separate XRD and XRF cells (Fig. 1).

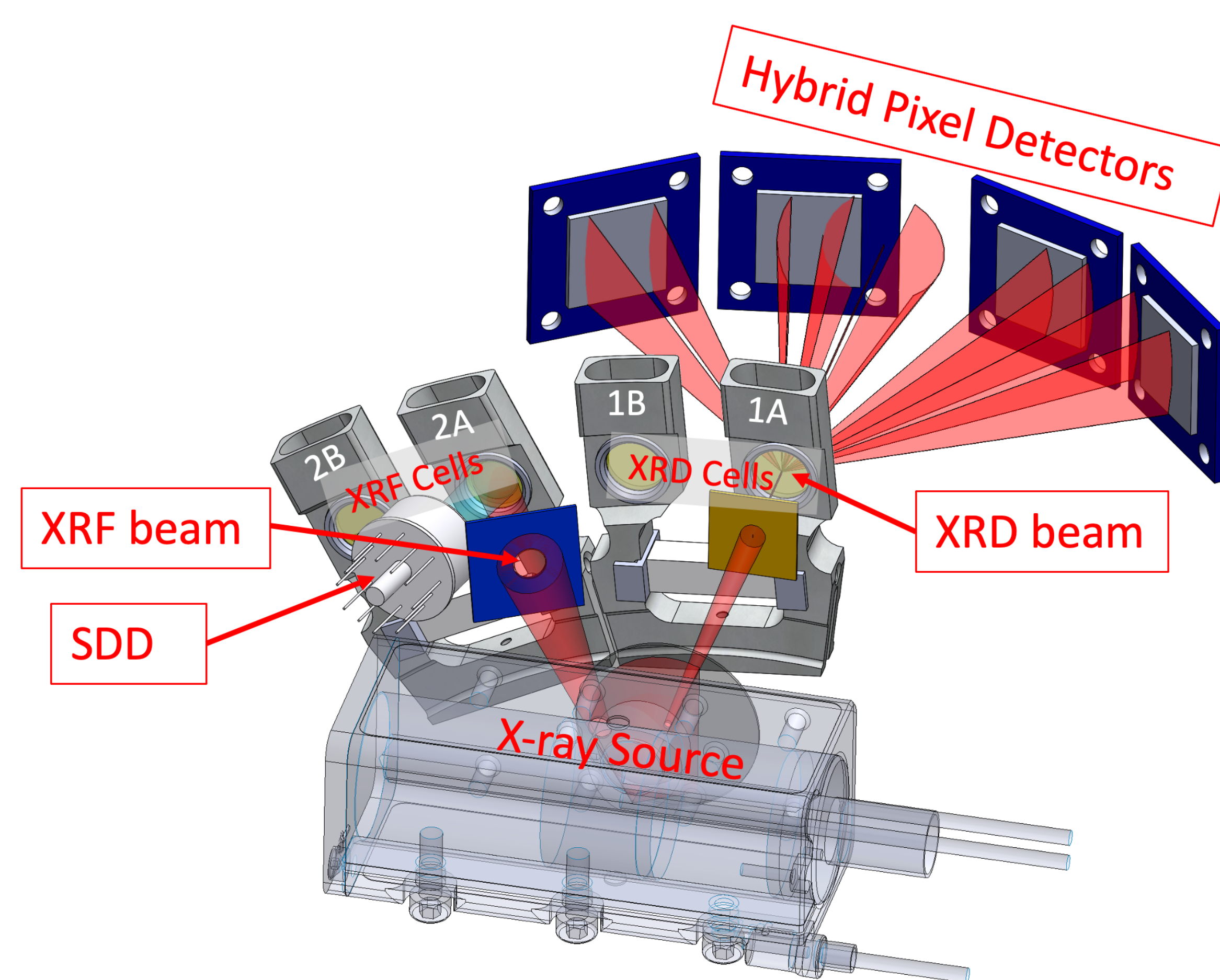


Fig. 1: Geometry of CheMin-V. A single X-ray source emits two separate beams, the first optimized for XRD and the second optimized for XRF.

## XRD geometry and XRD sample cell description:

The collimated X-ray beam from the source is directed through a thin layer (~175 μm) of <150 μm grain size Venus regolith confined between two 8 mm-diameter, 7 μm thick Kapton™ windows in the XRD sample cell (e.g., cell 1A in Fig. 1). The sample cell is shaken causing the loose powder to flow in a convection motion through the beam. The 2-D pattern collected by the detectors is summed circumferentially around the central beam to yield a conventional 1-D XRD pattern (Fig 2).

Fig. 2 shows an XRD pattern of Apollo 14 regolith sample 14149,26 collected in a 1-hour acquisition with a Terra™ XRD [3] (similar XRD geometry to CheMin-V) and quantified using Rietveld refinement [4] and whole pattern fitting [5]. Table 1 shows the resulting analysis.

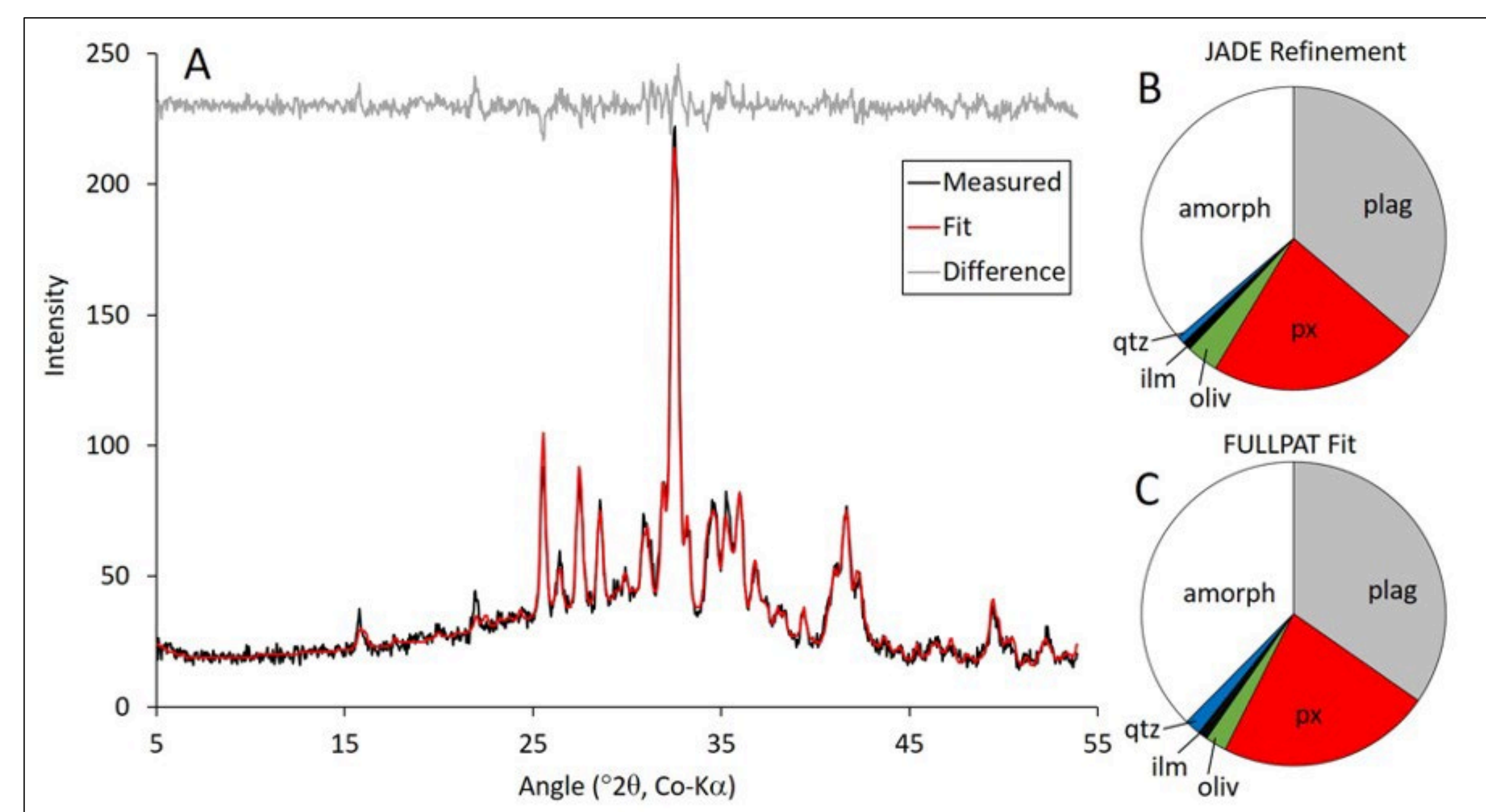


Fig 2: XRD pattern of <150 μm grainsize separate of Apollo 14 regolith sample 14149,26. Inset pie diagrams show proportions of crystalline and amorphous components determined using Rietveld refinement [4] and FULLPAT whole pattern fitting [5].

Table 1: Mineral Abundances and Compositions in Apollo 14 Regolith 14149,26

Mineral	Abundance <sup>1</sup>	Composition <sup>2</sup>
<b>Plagioclase Feldspar</b>	33.6 (0.8)	Ca <sub>0.94</sub> (4)Na <sub>0.06</sub> Al <sub>1.94</sub> Si <sub>2.06</sub> O <sub>8</sub>
<b>Augite</b>	7.1 (0.6)	Mg <sub>1.54</sub> (23)Ca <sub>0.63</sub> (11)Fe <sub>0.83</sub> (25)Si <sub>2</sub> O <sub>6</sub>
<b>Orthopyroxene</b>	8.5 (0.7)	Mg <sub>1.27</sub> (6)Fe <sub>0.61</sub> (6)Ca <sub>0.12</sub> (2)Si <sub>2</sub> O <sub>6</sub>
<b>Pigeonite</b>	7.3 (0.7)	Mg <sub>1.26</sub> (20)Fe <sub>0.53</sub> (21)Ca <sub>0.21</sub> (7)Si <sub>2</sub> O <sub>6</sub>
<b>Olivine</b>	3.5 (0.4)	Mg <sub>1.46</sub> (10)Fe <sub>0.54</sub> SiO <sub>4</sub>
<b>Quartz</b>	0.9 (0.1)	SiO <sub>2</sub>
<b>Ilmenite</b>	1.0 (0.2)	FeTiO <sub>3</sub>
<b>X-ray Amorphous</b>	38.0 (6.0)	in combination with XRF data <sup>3</sup>
<b>Total</b>	99.7	

<sup>1</sup>Values in parentheses are 1σ errors. <sup>2</sup>Calculated from unit-cell parameters [6] refined using MDI-JADE™. <sup>3</sup>The composition of the X-ray amorphous component can be determined by subtracting the composition of the crystalline component (derived from unit cell parameters) from the bulk composition (obtained from the XRF measurement).

**Hybrid Pixel Detectors for XRD:** Hybrid Pixel Detectors do not require cooling and can operate under high flux conditions (Fig 3). In a configuration like Fig. 1, this results in decreased analysis times and improved 2θ resolution along with much reduced power requirements. An array of 4 HPDs increases the 2θ resolution from 0.3° to 0.18°, sufficient to identify and quantify 3-pyroxene systems.

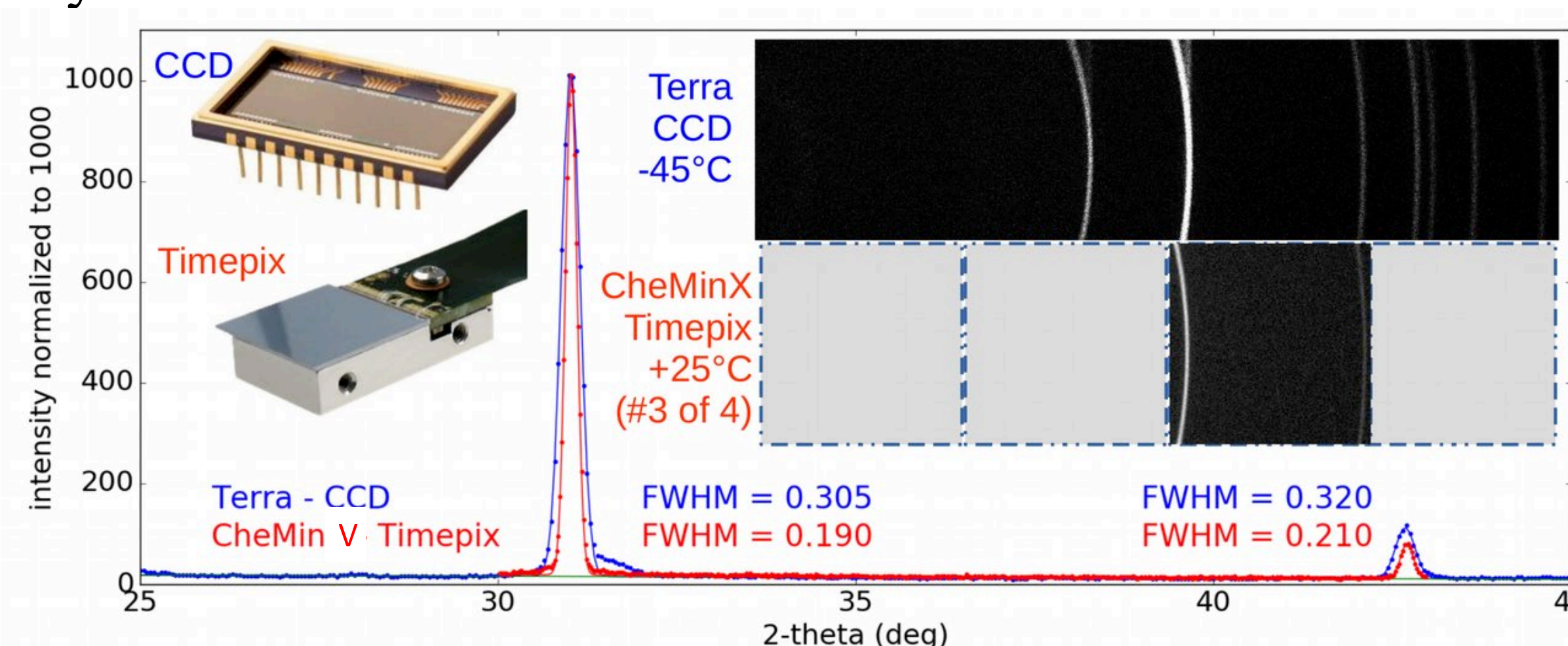


Fig 3: Comparison of XRD data of quartz using a CCD based Terra [3] vs. a HPD detector placed twice as far from the sample. HPDs don't require cooling; the CCD must be hermetically sealed in a chamber and cooled to -45°C. This preliminary measurement verifies the improved resolution of CheMinV.

**XRF geometry and sample cell description:** A divergent X-ray beam from the source fluoresces the XRF sample cell (e.g., cell 2A in Fig. 1) which is 8 mm in diameter and 3 mm thick. XRF data are collected with a silicon drift detector (SDD) placed in reflection geometry.

**Predicted XRF performance of CheMin-V:** Fundamental Parameters calculations [7] and Monte Carlo methods [8] were used to model the XRF performance of CheMin-V. Table 2 shows the calculated quantification and detection limits for select major, minor and trace elements in a basaltic or rhyolitic matrix.

Table 2. Quantification & Detection Limits in Basaltic or Rhyolitic Matrices Using XRF<sup>1,2</sup>

(Major Elements)				(Zr, Selected REE and Th)			
Z	Element	Quant. Limit (μg/g)	Det. Limit (μg/g)	Z	Element	Quant. Limit (μg/g)	Det. Limit (μg/g)
11	Na	592	178	40	Zr	10	3
12	Mg	239	72	57	La	10	3
13	Al	117	36	58	Ce	15	5
14	Si	86	26	60	Nd	6	2
15	P	72	22	62	Sm	5	2
16	S	28	9	63	Eu	51	16
17	Cl	21	7	64	Gd	42	13
19	K	6	2	66	Dy	119	36
20	Ca	7	2	68	Er	158	48
22	Ti	6	2	70	Yb	25	8
24	Cr	3	1	71	Lu	24	7
25	Mn	2	1	90	Th	17	5
26	Fe	8	3				

<sup>1</sup> Based on 1 hour of analysis

<sup>2</sup> These are "best case" values that do not take into account peak interferences. "Real world" detection and quantification limits in some cases will be higher, as for example Na or Mg in the presence of abundant Al.

**Discussion:** CheMin-V meets or exceeds the requirements of six investigations described in the "Scientific GOI for Venus Exploration" [9] that pertain to measurements of Venus surface chemistry and mineralogy: I. A. Hydrous Origins (1); I. A. Recycling (1); III. A. Geochemistry (1); III. B. Local Weathering (1); III. B. Global Weathering (2); and III. B. Chemical Interactions (3). XRD and XRF are listed as payload elements of the Venus Flagship Lander in the 2023-2032 Planetary Decadal Survey report [10].

**Acknowledgements:** This work was funded under NASA's PICASSO (#13-PICASSO13\_0111), MatISSE #16-MATISE16\_2-0005) and DALI (#18-DALI18\_2-0006) programs to DFB.

**References:** [1] Zacny et al. (2014), *IEEE Aerospace Conference*, 3-7 March, Big Sky MT. [2] Blake et al. (2012), *Space Sci. Rev.*, 10.1007/s11214-012-9905-1. [3] Sarrazin et al. (2008), *LPSC 39*, #2421. [4] Bish & Post (1993), *Am. Min.* **78**, 932-942. [5] Chipera & Bish (2002), *J. App. Cryst.*, **35**, 744-749. [6] Morrison et al., (2018), *Am. Min.*, 10.2138/am-2018-6123. [7] Sole' et al., (2007), *Spectrochim. Acta Part B*, **62**, 63-68. [8] Schoonjans et al. (2012) *Spectrochim. Acta Part B*, **70**, 10-23. [9] GOI for Venus Exploration (2019). [10] Planetary Decadal Survey 2023-2032, p. C12.